RSC Advances

PAPER

View Article Online
View Journal | View Issue



Cite this: *RSC Adv.*, 2026, **16**, 16156

# Thermodynamic analysis of the decomposition of scheelite by oxalic acid

Ting Xie,[ad] Jisen Huang,[a] Bin Zeng,*[ab] Xiangrong Zeng,*[ab] Chong Peng[a] and Zhonghua Wang[c]

The equilibrium diagram of the Ca–W–Oa–$H_2O$ system for the $H_2C_2O_4$ leaching of scheelite at 298 K was constructed. This diagram clarifies the dominant regions of each component in the system as well as the variation rules of key components with pH value and total concentration of free $H_2C_2O_4$, thereby confirming the thermodynamic conditions for the $H_2C_2O_4$ leaching of scheelite. Theoretical analysis results indicate that $H_2C_2O_4$ can effectively leach scheelite, and the concentration of $H_2C_2O_4$ is a crucial factor influencing the leaching efficiency. When 1 < pH < 6.4, scheelite reacts with $H_2C_2O_4$ to form precipitates of $H_2WO_{4(s)}$ and $CaC_2O_{4(s)}$. Under the condition of maintaining a high concentration of free $H_2C_2O_{4(aq)}$, $H_2WO_{4(s)}$ further reacts with $H_2C_2O_{4(aq)}$, and the formation of $H_2[WO_3(C_2O_4 \cdot H_2O)]$ with high solubility is predicted, which promotes the leaching of scheelite. When 6.4 < pH < 14.6, the ionization of $H_2C_2O_4$ is enhanced with the increase of pH, leading to the rise in the concentrations of $C_2O_4^{2-}$ and $WO_4^{2-}$. When pH > 14.6, the binding effect between $OH^-$ and $Ca^{2+}$ in the system is sharply strengthened, and $CaC_2O_{4(s)}$ is gradually converted into $Ca(OH)_{2(s)}$. Based on the thermodynamic analysis results, experimental verification of $H_2C_2O_4$ leaching of scheelite was carried out. Under the optimal conditions of $H_2C_2O_4$ concentration of 2.2 mol $L^{-1}$, reaction temperature of 80 °C, reaction time of 5 h, liquid-to-solid ratio of 15 : 1, and stirring speed of 100 rpm, the leaching rate of $WO_3$ reached 99.54%, with only 0.53% of $WO_3$ remaining in the leaching residue. Comparison of the XRD, EDS, and FTIR characterization results of raw scheelite and oxalic acid-leached residue reveals that during the leaching process, most of the tungsten enters the leachate in a highly soluble form, while calcium combines with $C_2O_4^{2-}$ to form $CaC_2O_4 \cdot H_2O$ precipitate, which is retained in the leaching residue.

Received 9th February 2026
Accepted 16th March 2026

DOI: 10.1039/d6ra01141a

rsc.li/rsc-advances



## 1 Introduction

Tungsten exhibits excellent physicochemical properties and boasts an extremely extensive range of industrial applications, serving as an irreplaceable critical metal.[1–3] At present, the mineral raw materials for tungsten smelting are mainly scheelite, wolframite, and mixed scheelite-wolframite ores. Among these, scheelite accounts for more than two-thirds of the global tungsten ore reserves, thus occupying a dominant position.[4,5] How to achieve the high-efficiency utilization of scheelite has become a pivotal issue that urgently needs to be addressed in the tungsten smelting industry.

The smelting processes for scheelite mainly include the high-dose alkali autoclave decomposition method, sodium carbonate autoclave decomposition method, mixed sulfuric-phosphoric acid decomposition method, and hydrochloric acid decomposition method.[6–15] Among these, the high-dose alkali autoclave decomposition method has broken the theoretical bottleneck that sodium hydroxide cannot decompose scheelite and realized the efficient decomposition of scheelite, yet it suffers from a relatively high consumption of sodium hydroxide.[6–9] The sodium carbonate autoclave decomposition method is capable of treating low-grade complex scheelite under the conditions of high temperature and high pressure (temperature: 180–220 °C, pressure: 1.6–2.2 MPa), with the tungsten content in the decomposition residue stably controlled at ≤ 0.6%, but it is associated with high energy consumption.[10,11] The mixed sulfuric-phosphoric acid decomposition method introduces phosphoric acid as a strong complexing agent, which enables the efficient decomposition of scheelite under atmospheric pressure at 80–90 °C and has been industrialized.[12,13] Although the hydrochloric acid decomposition method features high treatment efficiency, it causes severe corrosion to equipment and involves great difficulty in the treatment of acid-decomposed mother liquor, which restricts its practical application.[14,15]

To achieve more efficient and greener utilization of scheelite, researchers have developed novel decomposing agents for

[a]College of Intelligent Manufacturing and Materials Engineering, Gannan University of Science and Technology, Ganzhou 341000, China. E-mail: Zengbin@163.com; zengxr986@163.com
[b]Jiangxi Yaosheng Tungsten Co., Ltd, Ganzhou 341000, China
[c]Ganzhou Juxin Mining Co., Ltd, Ganzhou 341000, China
[d]Jiangxi Vocational College of Environmental Engineering, Ganzhou 341000, China

scheelite, with significant progress attained.[16–19] Sodium phytate-sulfuric acid acts as a decomposing agent for scheelite, yielding a high decomposition rate under atmospheric pressure and heating conditions, phytic acid exhibits excellent complexing performance for tungsten, yet its industrial application awaits further investigation.[16] Sulfuric acid-hydrogen peroxide serves as a scheelite decomposing agent, in which hydrogen peroxide is used to complex and dissolve the formed tungstic acid. This system achieves a high decomposition rate under a high liquid-to-solid ratio, but impurities are prone to simultaneous leaching.[17] For the synergistic decomposition of scheelite by sulfuric acid-oxalic acid, sulfuric acid reacts with calcium to form calcium sulfate precipitate that enters the decomposition residue, while $H_2C_2O_4$ fulfills the function of tungsten complexation. Tungsten then enters the decomposition solution in the form of highly soluble $H_2[WO_3(C_2O_4)\cdot H_2O]$.[18,19] In summary, the adoption of complex leaching technology, *via* the introduction of complexing agents to facilitate the formation of soluble tungsten complexes, can effectively overcome the kinetic limitations in the scheelite leaching process.

Oxalic acid ($H_2C_2O_4$), the simplest dicarboxylic acid, can not only form the highly soluble complex $H_2[WO_3(C_2O_4)\cdot H_2O]$ with tungsten in scheelite but also generate the precipitate $CaC_2O_4$ with calcium in scheelite, thus serving as a potential high-efficiency novel decomposing agent for scheelite.[20,21] However, existing studies on $H_2C_2O_4$ leaching of scheelite have focused merely on process optimization, and systematic investigations into the thermodynamic equilibrium laws, distribution characteristics of various components and reaction mechanisms of the Ca–W–Oa–$H_2O$ system remain rather scarce. This deficiency leads to the lack of theoretical guidance for the optimization of process parameters, thereby restricting the industrial application of this technology. Based on this, the present study intends to conduct thermodynamic calculations for the $H_2C_2O_4$ leaching process of scheelite, establish the equilibrium relationships of the Ca–W–Oa–$H_2O$ system, and plot the lg[M]–pH diagrams under different conditions. The influence laws of key parameters such as pH value and $H_2C_2O_4$ concentration on the species distribution of tungsten and calcium as well as the leaching efficiency of scheelite are systematically analyzed, and the thermodynamic conditions for the complex leaching of scheelite with $H_2C_2O_4$ are clarified, which is expected to provide a theoretical reference for the development of a new scheelite decomposition process.

## 2 Thermodynamic calculations and equilibrium diagram plotting

### 2.1 Thermodynamic data

The equilibrium reactions existing in the solution system and their corresponding data sources are presented in Table 1.

### 2.2 Thermodynamic calculations

Based on the equilibria existing in the system listed in Table 1, thermodynamic calculations can be performed starting from the total concentrations of free calcium, free tungsten and free $H_2C_2O_4$, with the concentration of each dissolved component in the solution denoted as [M]. In addition, $H_2C_2O_4$ can form complex coordination compounds with tungstic acid, and relevant details have not been reported to date. Therefore, only the currently available thermodynamic data were adopted for the investigation and analysis. In cases where the activity coefficients of relevant ions were unavailable, concentrations were used as substitutes for all calculations.[24]

Let the total concentration of free tungsten in the system be defined as [W], with its existing species in the solution including $WO_4^{2-}$, $HWO_4^-$ and $H_2WO_{4(aq)}$. Based on the equilibrium relationships (I), (II), (IX) listed in Table 1 and the principle of mass conservation, their corresponding equilibrium concentrations satisfy the following relationship:

$$[W] = [WO_4^{2-}] + [HWO_4^-] + [H_2WO_{4(aq)}] \quad (1)$$

$$[HWO_4^-] = 1 \times 10^{3.5}[H^+][WO_4^{2-}] \quad (2)$$

$$[H_2WO_{4(aq)}] = 1 \times 10^{8.1}[H^+]^2[WO_4^{2-}] \quad (3)$$

Let the total concentration of free $H_2C_2O_4$ in the system be defined as [Oa], with its existing species in the solution including $C_2O_4^{2-}$, $HC_2O_4^-$, $H_2C_2O_4$ and $CaC_2O_{4(aq)}$. Based on the equilibrium relationships (VI), (V), (VII) listed in Table 1 and the principle of mass conservation, their corresponding equilibrium concentrations satisfy the following relationship:

$$[Oa] = [C_2O_4^{2-}] + [HC_2O_4^-] + [H_2C_2O_4] + [CaC_2O_{4(aq)}] \quad (4)$$

$$[HC_2O_4^-] = 1 \times 10^{4.272}[H^+][C_2O_4^{2-}] \quad (5)$$

$$[H_2C_2O_4] = 1 \times 10^{5.543}[H^+]^2[C_2O_4^{2-}] \quad (6)$$

$$[CaC_2O_{4(aq)}] = 1 \times 10^{3.0}[Ca^{2+}][C_2O_4^{2-}] \quad (7)$$

Let the total concentration of free calcium in the system be defined as [Ca], with its existing species in the solution including $Ca^{2+}$, $CaOH^+$, $Ca(OH)_{2(aq)}$ and $CaC_2O_{4(aq)}$. Based on the equilibrium relationships (III), (XI), (XII) listed in Table 1 and the principle of mass conservation, their corresponding equilibrium concentrations satisfy the following relationship:

$$[Ca] = [Ca^{2+}] + [CaOH^+] + [Ca(OH)_{2(aq)}] + [CaC_2O_{4(aq)}] \quad (8)$$

$$[CaOH^+] = 1 \times 10^{-12.75}[Ca^{2+}]/[H^+] \quad (9)$$

$$[Ca(OH)_{2(aq)}] = 1 \times 10^{-25.23}[Ca^{2+}]/[H^+]^2 \quad (10)$$

$$[CaC_2O_{4(aq)}] = 1 \times 10^{3.0}[Ca^{2+}][C_2O_4^{2-}] \quad (11)$$

Within the stability regions of the corresponding species, the relevant ions satisfy the following dissolution equilibria:

Since this study requires scheelite to be in an excess state in the Ca–W–Oa–$H_2O$ system, the dissolution equilibrium of $CaWO_4$ is maintained throughout the entire experimental investigation range. From the equilibrium equation (VIII), it can be derived that:

Table 1 Equilibrium reaction and equilibrium constant in Ca–W–Oa–$H_2O$ system (25 °C)[22,23]

| No. | Equilibrium reaction | lg $K$ | Balance equation |
|---|---|---|---|
| I | $H_2WO_{4(aq)} = H^+ + HWO_4^-$ | −4.60 | $[H^+] \times [HWO_4^-] \times [H_2WO_{4(aq)}]^{-1} = 10^{-4.6}$ |
| II | $HWO_4^- = H^+ + WO_4^{2-}$ | −3.50 | $[H^+] \times [WO_4^{2-}]*[HWO_4^-]^{-1} = 10^{-3.5}$ |
| III | $H_2O = H^+ + OH^-$ | −13.99 | $[H^+] \times [OH^-] = 10^{-13.99}$ |
| IV | $CaC_2O_4 \cdot H_2O_{(s)} = Ca^{2+} + C_2O_4^{2-} + H_2O$ | −8.63 | $[Ca^{2+}] \times [C_2O_4^{2-}] = 10^{-8.63}$ |
| V | $H_2C_2O_4 = HC_2O_4^- + H^+$ | −1.27 | $[H^+] \times [HC_2O_4^-] \times [H_2C_2O_4]^{-1} = 10^{-1.27}$ |
| VI | $HC_2O_4^- = C_2O_4^{2-} + H^+$ | −4.27 | $[H^+] \times [C_2O_4^{2-}] \times [HC_2O_4^-]^{-1} = 10^{-4.27}$ |
| VII | $CaC_2O_{4(aq)} = Ca^{2+} + C_2O_4^{2-}$ | −3.0 | $[Ca^{2+}] \times [C_2O_4^{2-}] \times [CaC_2O_{4(aq)}]^{-1} = 10^{-3}$ |
| VIII | $CaWO_{4(s)} = Ca^{2+} + WO_4^{2-}$ | −8.80 | $[Ca^{2+}] \times [WO_4^{2-}] = 10^{-8.8}$ |
| IX | $H_2WO_{4(s)} = 2H^+ + WO_4^{2-}$ | −15.80 | $[H^+]^2 \times [WO_4^{2-}] = 10^{-15.8}$ |
| X | $Ca(OH)_{2(s)} = Ca^{2+} + 2OH^-$ | −5.26 | $[Ca^{2+}] \times [OH^-]^2 = 10^{-5.26}$ |
| XI | $Ca(OH)_{2(aq)} = Ca^{2+} + 2OH^-$ | −2.77 | $[Ca^{2+}] \times [OH^-]^2 \times [Ca(OH)_{2(aq)}] = 10^{-2.77}$ |
| XII | $CaOH^+ = Ca^{2+} + OH^-$ | −1.23 | $[Ca^{2+}] \times [OH^-] \times [CaOH^+] = 10^{-1.23}$ |

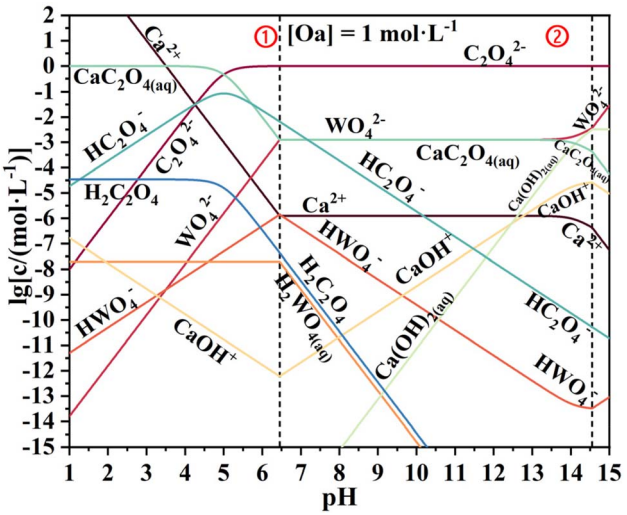


Fig. 1 Lg[M]–pH diagram for solution species in the Ca–W–Oa–$H_2O$ system ([Oa] = 1 mol $L^{-1}$).

$$[Ca^{2+}][WO_4^{2-}] = 10^{-8.8} \quad (12)$$

When $H_2WO_{4(s)}$ is formed in the Ca–W–Oa–$H_2O$ system, it can be derived from equilibrium equations (I), (II) and (IX) that:

$$[H^+]^2[WO_4^{2-}] = 10^{-14.78} \quad (13)$$

$$[H_2WO_{4(aq)}] = 10^{-6.68} \quad (14)$$

When only $CaWO_{4(s)}$ exists as the solid phase in the Ca–W–Oa–$H_2O$ system, all ions in the solution are provided by $CaWO_{4(s)}$, which should satisfy the following relationship:

$$[Ca] = [W] \quad (15)$$

When $CaC_2O_4 \cdot H_2O_{(s)}$ is formed in the Ca–W–Oa–$H_2O$ system, it can be derived from equilibrium equations (IV) and (VII) that:

$$[Ca^{2+}][C_2O_4^{2-}] = 10^{-8.63} \quad (16)$$

$$[CaC_2O_{4(aq)}] = 10^{-5.63} \quad (17)$$

when $Ca(OH)_{2(s)}$ is formed in the Ca–W–Oa–$H_2O$ system, it can be derived from equilibrium equations (III) and (X) that:

$$[Ca^{2+}] = 10^{22.74}[H^+]^2 \quad (18)$$

### 2.3 Calculation and discussion of stability region boundaries

According to relevant literature, the calculation and discussion of the thermodynamic stability region boundaries for the $H_2C_2O_4$ leaching of scheelite in this paper refer to the calculation and discussion methods of the fluoride salt decomposition system,[25] silicate decomposition system,[26] phosphate/ammonium phosphate decomposition system,[27] sodium carbonate system,[28] EDTA decomposition system,[29] and other related systems. By comparing the solubility products of $CaC_2O_4$ and $Ca(OH)_2$ listed in Table 1, it can be concluded that the solubility product of $CaC_2O_4$ is much smaller than that of $Ca(OH)_2$, indicating that $CaC_2O_4$ has a greater tendency to form precipitates than $Ca(OH)_2$ under the same conditions. Meanwhile, since $Ca^{2+}$ and $C_2O_4^{2-}$ released from calcium tungstate already exist in the system, the condition $Q_c = [Ca^{2+}][C_2O_4^{2-}] > K_{sp}(CaC_2O_4)$ can be satisfied even at a relatively low $OH^-$ concentration. ($Q_c = [Ca^{2+}][C_2O_4^{2-}]$) refers to the product of the molar concentrations of calcium ions and oxalate ions in the system, which is a real-time dynamic value and varies with the changes in ion concentrations in the reaction system. $K_{sp}$($CaC_2O_4$) denotes the product of the molar concentrations of the ions in the solution when calcium oxalate reaches the dissolution–precipitation equilibrium under a given set of conditions, and it is a thermodynamic constant. In summary, the system for the $H_2C_2O_4$ leaching of scheelite can be divided into three stability regions: the $H_2WO_4$ stability region, $CaC_2O_4$ + $CaWO_4$ stability region, and $Ca(OH)_2$ stability region.

The initial free oxalate concentration [Oa] in the Ca–W–Oa–$H_2O$ system was set to 1 mol $L^{-1}$. In the stability region of $CaWO_4$, both $Ca^{2+}$ and $WO_4^{2-}$ in the system are derived from $CaWO_4$, and eqn (1)–(12) and (15) must be satisfied simultaneously. Under the boundary conditions for the transformation of $CaWO_4$ to $H_2WO_4$, eqn (1)–(15) must be satisfied

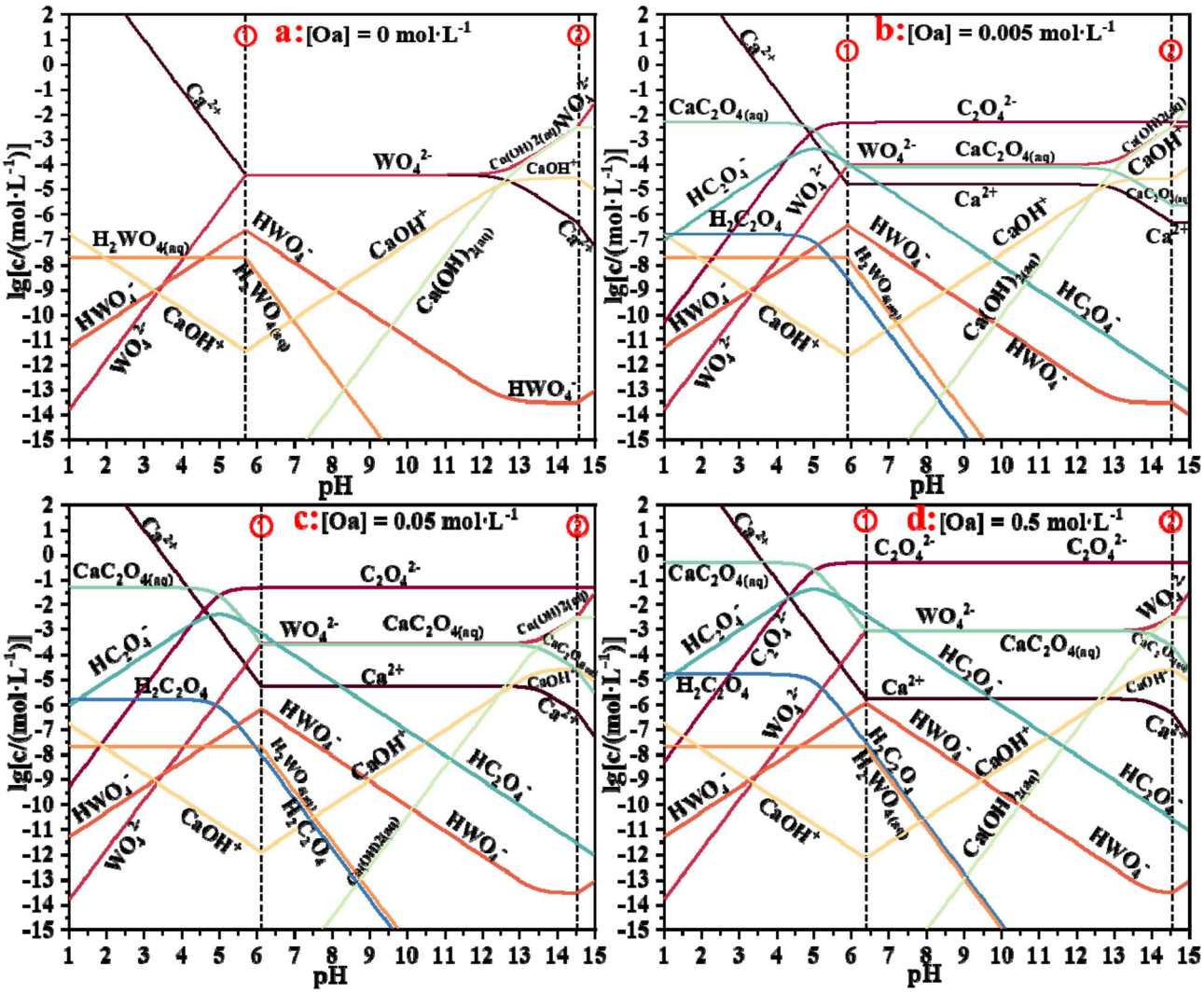


Fig. 2 Lg[M]–pH diagrams for solution species in the Ca–W–Oa–$H_2O$ system (a: [Oa] = 0 mol L; b: [Oa] = 0.005 mol L; c: [Oa] = 0.05 mol L; d: [Oa] = 0.5 mol $L^{-1}$).

simultaneously. In the stability regions of $CaC_2O_4$ + $CaWO_4$ and at the boundary of the $Ca(OH)_2$ stability region, eqn (1)–(12) and (15)–(18) must be satisfied simultaneously.

The dissolution equilibria of various species in the system were calculated using the methods of classified discussion and univariate solution, and the relationship diagrams between the logarithm of species concentration lg[M] and pH value were thus obtained, as presented in Fig. 1. In addition, the dissolution equilibria of solution species were calculated separately at different oxalate concentrations ([Oa] = 0 mol $L^{-1}$, 0.005 mol $L^{-1}$, 0.05 mol $L^{-1}$, and 0.5 mol $L^{-1}$) using the same computational method, with the results shown in Fig. 2. The relationship diagrams of the logarithm of total tungsten concentration lg[W] *versus* pH (lg[W]–pH diagrams) under different oxalate concentrations [Oa] were also plotted, as illustrated in Fig. 3. To further explore the influence of oxalate concentration on the leaching behavior of scheelite, the relationship diagrams of lg[M] *versus* oxalate concentration (lg[M]–lg[$H_2C_2O_4$] diagrams) were constructed, as displayed in Fig. 4.

### 2.4 Thermodynamic condition analysis of the Ca–W–Oa–$H_2O$ system

Fig. 1 shows the lg[M]–pH diagram plotted at an oxalate concentration [Oa] = 1 mol $L^{-1}$. The region to the left of dashed line ① is the stability region of tungstic acid, which corresponds to the acidic leaching process of calcium tungstate, with $H_2WO_4$ as the main solid product. The region between dashed line ① and dashed line ② is the stability region for the $CaC_2O_4$ + $CaWO_4$. The region to the right of dashed line ② is the stability region of $Ca(OH)_2$.

Within the stability region of $H_2WO_4$ (1 < pH < 6.4), the acidic leaching of calcium tungstate dominates, with $H_2WO_4$ as the main solid product. $H_2C_2O_4$ is a weak diprotic acid. At low pH, the high $H^+$ concentration in the system suppresses the dissociation of $H_2C_2O_4$, resulting in a relatively high $H_2C_2O_4$ concentration. As pH increases, the $H^+$ concentration decreases, and equilibrium equations (V) and (VI) proceed forward, leading to a declining trend in $H_2C_2O_4$ concentration.

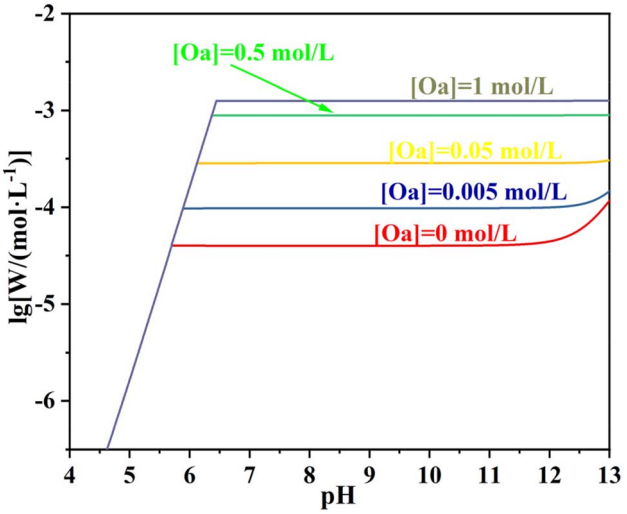


Fig. 3 Lg[W (mol$^{-1}$ L$^{-1-1}$)]–pH diagram for solution species in the Ca–W–Oa–$H_2O$ system.

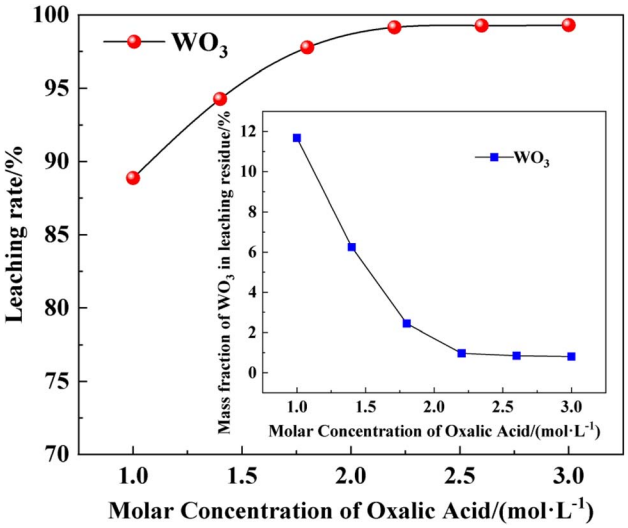


Fig. 5 Effect of $H_2C_2O_4$ molar concentration on the leaching rate of $WO_3$ in scheelite.

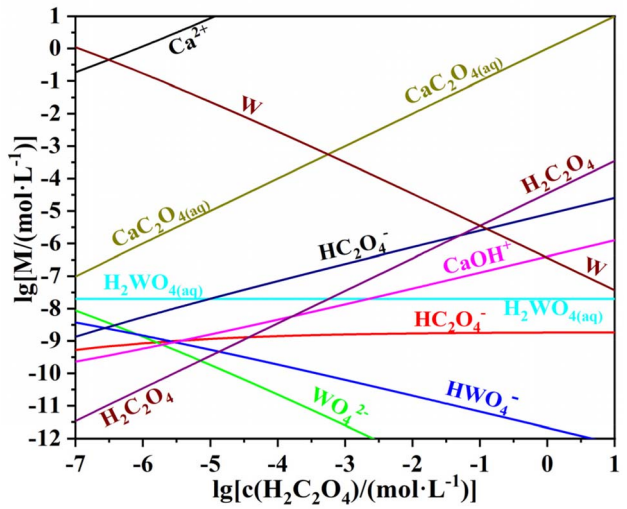


Fig. 4 Lg[M]–lg[c($H_2C_2O_4$)] diagram for solution species in the Ca–W–Oa–$H_2O$ system.

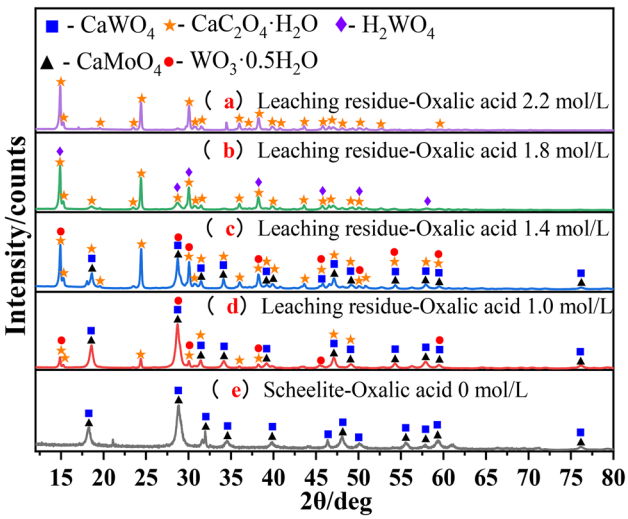


Fig. 6 The X-ray patterns of leaching residues at different molar concentrations of oxalic acid, (a) 2.2 mol L; (b) 1.8 mol L; (c) 1.4 mol L; (d) 1.0 mol L; (e) 0 mol L$^{-1}$.

According to equation (V), the gradual dissociation of $H_2C_2O_4$ with rising pH gives rise to an increasing trend for $HC_2O_4^-$. However, as pH increases further, equation (VI) shifts forward to produce $C_2O_4^{2-}$, so the $C_2O_4^{2-}$ concentration increases continuously, while the $HC_2O_4^-$ concentration begins to decrease. Therefore, within the $H_2WO_4$ stability region, the $HC_2O_4^-$ concentration first increases and then decreases with increasing pH.

During the $H_2C_2O_4$ leaching of calcium tungstate under acidic conditions, $H_2WO_{4(s)}$ is formed. The dissolution equilibrium of $H_2WO_4$ in solution brings $H_2WO_{4(aq)}$ to its equilibrium level. As pH decreases, the $H^+$ concentration in the system increases, and equations (I), (II), and (IX) all proceed in the reverse direction, strengthening the tendency to form $H_2WO_{4(s)}$. Consequently, the concentrations of $HWO_4^-$ and $WO_4^{2-}$ in the system both decrease. Under these conditions, if the system contains a high concentration of $H_2C_2O_{4(aq)}$, $H_2WO_{4(s)}$ will further undergo a complexation reaction with $H_2C_2O_{4(aq)}$ to form the highly soluble complex $H_2[WO_3[C_2O_4 \cdot H_2O]]$, based on reported literature results.[18,19]

Within the stability region of $CaC_2O_4$ + $CaWO_4$ (6.4 < pH < 14.6), the dissociation tendency of $H_2C_2O_4$ and $HC_2O_4^-$ increases with rising pH, and the concentrations of $H_2C_2O_4$ and $HC_2O_4^-$ both decrease linearly. The concentration of $HC_2O_4^-$ gradually decreases with increasing pH, whereas the concentration of $C_2O_4^{2-}$ increases continuously as $H_2C_2O_4$ dissociates more completely, making $C_2O_4^{2-}$ the dominant species of $H_2C_2O_4$. With increasing pH, $H_2WO_4$ and $HWO_4^-$ are almost fully dissociated, and their concentrations decrease

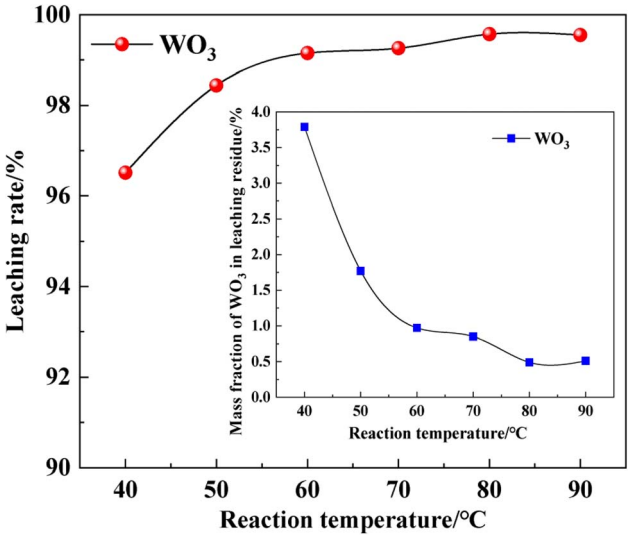


Fig. 7 Effect of reaction temperature on the leaching rate of $WO_3$ in scheelite.

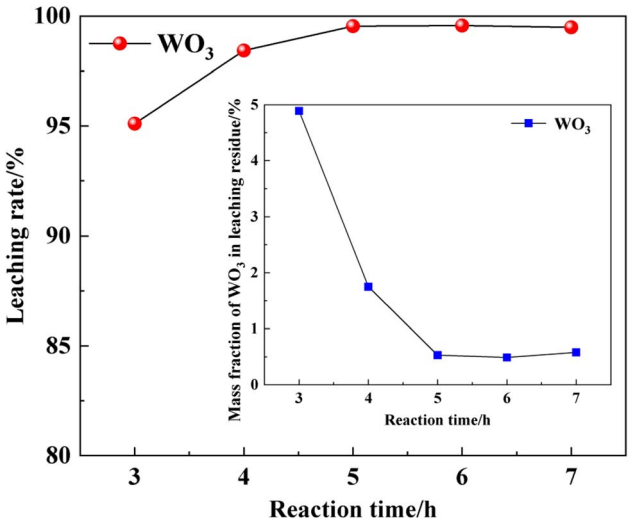


Fig. 8 Effect of reaction time on the leaching rate of $WO_3$ in scheelite.

continuously to extremely low levels. Meanwhile, the $WO_4^{2-}$ concentration reaches a steady state and becomes the predominant species of tungsten. As pH increases, $Ca^{2+}$ gradually combines with $OH^-$ to form $Ca(OH)_{2(aq)}$ and $CaOH^+$, so the $Ca^{2+}$ concentration exhibits a decreasing trend.

Within the stability region of $Ca(OH)_2$ (pH > 14.6), both $CaWO_4$ and $CaC_2O_4$ are transformed into $Ca(OH)_{2(s)}$. The increasing $OH^-$ content in the system enhances the binding ability of $OH^-$, which intensifies the extraction of $Ca^{2+}$ from $CaWO_4$ and $CaC_2O_4$ to form $Ca(OH)_{2(s)}$. At the same time, $OH^-$ also combines with free $Ca^{2+}$ to form precipitates. Consequently, the concentration of $WO_4^{2-}$ in the system shows an increasing trend, while the concentrations of $CaC_2O_{4(aq)}$ and $Ca^{2+}$ both decrease. The formation of $Ca(OH)_{2(s)}$ simultaneously brings $Ca(OH)_{2(aq)}$ to its dissolution equilibrium.

To further explore the mechanism of scheelite leaching by $H_2C_2O_4$, lg[M]–pH diagrams (Fig. 2), lg[W]–pH diagrams (Fig. 3), and lg[M]–lg[$H_2C_2O_4$] diagrams (Fig. 4) were plotted at $H_2C_2O_4$ concentrations of 0 mol $L^{-1}$, 0.005 mol $L^{-1}$, 0.05 mol $L^{-1}$, and 0.5 mol $L^{-1}$, respectively. Combining Fig. 2 and 3, it can be seen that increasing the dosage of $H_2C_2O_4$ during leaching can increase the concentration of $WO_4^{2-}$ in the system. As the $H_2C_2O_4$ concentration gradually increases, the boundary pH for the transformation of $CaWO_4$ to $H_2WO_4$ gradually increases. Therefore, the $H_2C_2O_4$ concentration is an important factor affecting the leaching of $CaWO_4$.

Analysis of Fig. 3 shows that at pH < 5, the variation trend of [W] is consistent in systems with different $H_2C_2O_4$ concentrations. When the $H_2C_2O_4$ concentration [Oa] = 0 mol $L^{-1}$, the [W] concentration in the system is $10^{-4.5}$ mol $L^{-1}$. When 0.005 mol $L^{-1}$, 0.05 mol $L^{-1}$, and 0.5 mol $L^{-1}$ $H_2C_2O_4$ are added, the [W] concentration in the system increases to approximately $10^{-4}$ mol $L^{-1}$, $10^{-3.5}$ mol $L^{-1}$, and $10^{-3}$ mol $L^{-1}$, respectively. The [W] content in the system is linearly correlated with the $H_2C_2O_4$ concentration. Accordingly, the $H_2C_2O_4$ concentration is confirmed to be a key factor influencing the leaching of $CaWO_4$.

To further analyze the influence of $H_2C_2O_4$ concentration on scheelite leaching, the lg[M]–lg[$H_2C_2O_4$] diagram was plotted (see Fig. 4). It can be seen from Fig. 4 that the $Ca^{2+}$ concentration shows a linear decreasing trend with the increase of $H_2C_2O_4$ concentration. This is because the increase in $H_2C_2O_4$ concentration leads to an increase in $C_2O_4^{2-}$ concentration, and $C_2O_4^{2-}$ is more likely to combine with $Ca^{2+}$ to form $CaC_2O_{4(aq)}$, thereby reducing the $Ca^{2+}$ concentration and increasing the $CaC_2O_{4(aq)}$ concentration in the system.

The concentration of $HC_2O_4^-$ increases with the increase of $H_2C_2O_4$, which is due to the fact that the dissociation equation of $H_2C_2O_4$ ($H_2C_2O_4 = H^+ + HC_2O_4^-$) is more likely to proceed forward with the increase of $H_2C_2O_4$ concentration. The concentration of $CaOH^+$ increases with the increase of $H_2C_2O_4$,

Table 2 Effect of reaction liquid to solid ratio on the leaching rate of $WO_3$ in scheelite

| Experiment number | Scheelite usage/g | Liquid to solid ratio | The mass of leaching residue/g | Mass fraction of $WO_3$ in leaching residue/% | Leaching rate of tungsten trioxide from scheelite/% |
|---|---|---|---|---|---|
| I | 10 | 5 : 1 | 6.95 | 9.79 | 88.52 |
| II | 10 | 10 : 1 | 6.15 | 4.69 | 95.13 |
| III | 10 | 15 : 1 | 5.35 | 0.54 | 99.51 |
| IV | 10 | 20 : 1 | 5.16 | 0.53 | 99.54 |
| V | 10 | 25 : 1 | 5.15 | 0.48 | 99.58 |

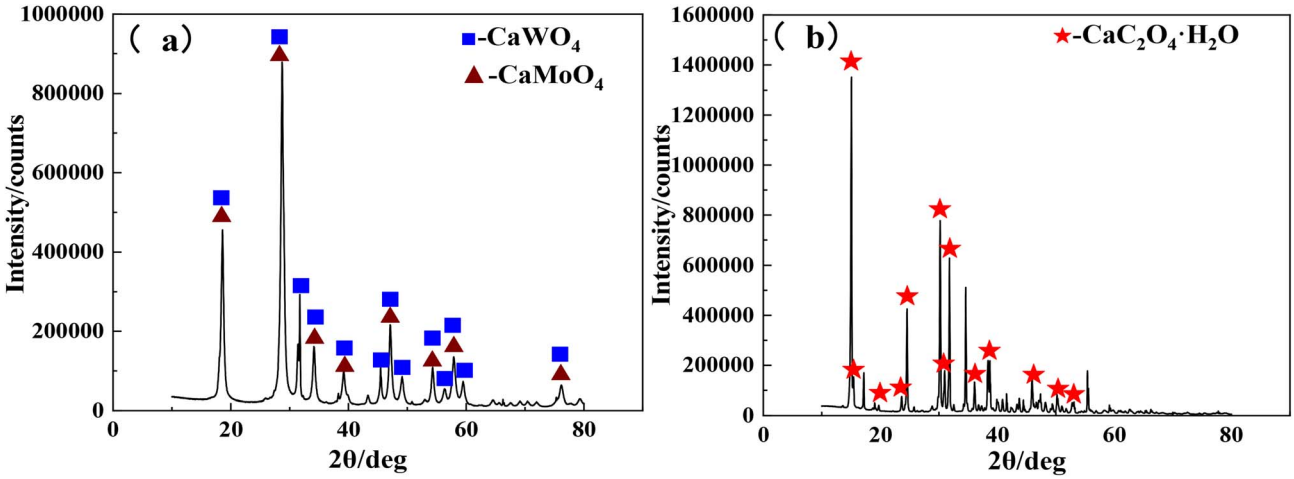


Fig. 9 The X-ray diffraction pattern: (a) scheelite; (b) $H_2C_2O_4$ leaching residue.

because the change in $H_2C_2O_4$ concentration affects the interaction between ions, promoting the tendency of $Ca^{2+}$ to combine with $OH^-$ to form $CaOH^+$.

The concentration of $WO_4^{2-}$ decreases with the increase of $H_2C_2O_4$, which is attributed to the increase of $H_2C_2O_4$ concentration in the system, leading to the formation of $H_2WO_{4(s)}$; meanwhile, $H_2WO_{4(s)}$ further reacts with $H_2C_2O_4$ to generate the highly soluble complex $H_2[WO_3[C_2O_4 \cdot H_2O]]$. The concentration of $HWO_4^-$ decreases with the increase of $H_2C_2O_4$, because a large amount of free $H^+$ is added to the system, which affects the dissociation equilibrium of $H_2WO_4$, prompting $HWO_4^-$ to convert to $H_2WO_{4(aq)}$, and $H_2WO_{4(aq)}$ further converts to $H_2WO_{4(s)}$.

In summary, the $H_2C_2O_4$ concentration is an important factor affecting the leaching effect of $CaWO_4$. Maintaining a relatively high concentration of $H_2C_2O_4$ in the system can promote the leaching of $CaWO_4$ and facilitate the dissolution of tungsten.

## 3 Experiment on leaching scheelite with oxalic acid

### 3.1 Experimental materials and methods

The raw material adopted in the experiment was high-grade scheelite (containing 59.25% $WO_3$, 2.63% Mo and 16.21% Ca), which was provided by a tungsten smelting enterprise in Ganzhou. The scheelite was first dried at 105 °C for 6 hours, then crushed by a ball mill. After crushing, the proportion of scheelite particles less than 45 μm was 100%, and finally the scheelite sample for the experiment was prepared. $H_2C_2O_4$ (AR

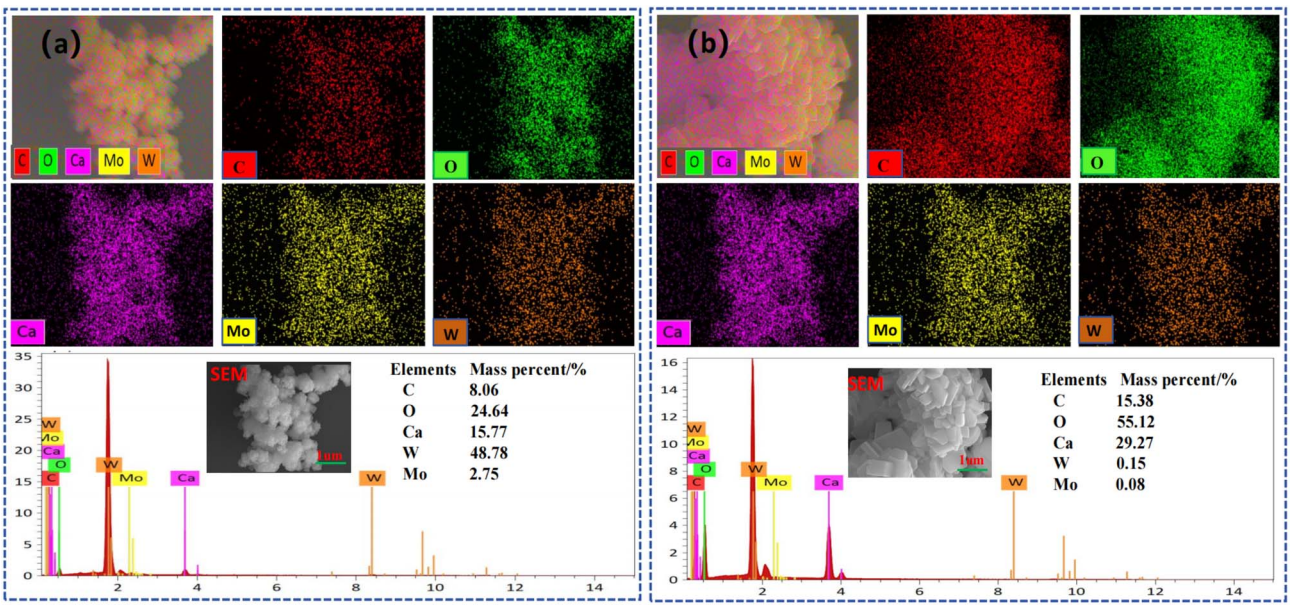


Fig. 10 Energy dispersive X-ray spectrometer pattern: (a) scheelite; (b) $H_2C_2O_4$ leaching residue.

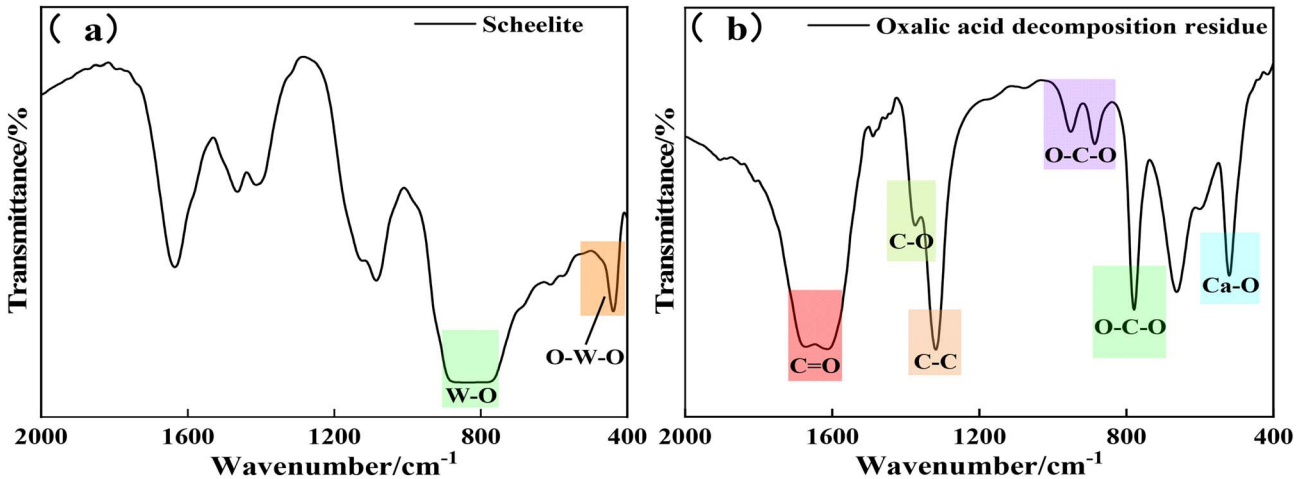


Fig. 11 Fourier transform infrared spectrometer spectrum pattern: (a) scheelite; (b) $H_2C_2O_4$ leaching residue.

grade, $C_2H_2O_4 \cdot 2H_2O \geq 99.0\%$) was used as the leaching agent, which was purchased from Xilong Scientific Co., Ltd. The pure water used in the experiment was prepared by a pure water machine.

Scheelite leaching experiment: weigh 10 g of scheelite and place it in an open glass beaker with a volume of 250 mL. Add an appropriate amount of pure water and $H_2C_2O_4$ as required by the experiment, and stir and mix (the stirring speed is controlled at 100 rpm). Place the glass beaker containing the scheelite slurry in a digital display constant temperature magnetic stirring water bath, and control the appropriate leaching temperature, stirring speed and stirring time. After the leaching reaction is completed, filter and wash the leaching slurry, collect and treat the filtrate and washing water. The washed leaching residue is dried in an oven at 105 °C for 6 hours. After the dried residue is cooled to room temperature, weigh it and prepare the leaching residue sample for chemical element analysis and phase analysis.

The calculation method of $WO_3$ leaching rate in scheelite is as follows:

$$\eta_W = \left(1 - \frac{m_a C_{aW}}{m_b C_{bW}}\right) \times 100\% \quad (19)$$

$\eta_W$ refers to the leaching rate of $WO_3$ in scheelite (%), $m_a$ refers to the weight of leaching residue (g), $m_b$ refers to the weight of scheelite concentrate used for leaching (g), $C_{aW}$ refers to the content of $WO_3$ in leaching residue (%), and $C_{bW}$ refers to the content of $WO_3$ in scheelite concentrate (%).

### 3.2 Experimental instruments

Experimental instruments: the instruments required for the scheelite leaching experiment are as follows: Pure Water Machine (Plain Series, Shanghai Yishuo Scientific Instruments Co., Ltd), X-ray Diffractometer (ULTIMA I, Rigaku), Energy Dispersive Spectrometer (X-MaxN50, Oxford Instrument EDS), Fourier Transform Infrared Spectrometer (Scientific Nicolet iN10, Thermofisher Scientific), X-ray Photoelectron Spectrometer (K-Alpha, Thermofisher Scientific), Digital Display Constant Temperature Magnetic Stirring Water Bath (DF-101S, ±0.5 °C, Shanghai Yuezhong Instrument Equipment Co., Ltd), Blast Drying Oven (JC101, ±0.5 °C, Shanghai Chengshun Instruments and Meters Co., Ltd), Electronic Balance (BS-600, ±0.001 g, Shanghai Yousheng Weighing Apparatus Co., Ltd), and Spectrophotometer (722N, Shanghai INESA Analytical Instruments Co., Ltd). The mass fraction of $WO_3$ in scheelite was determined according to the Chemical Analysis Method for Tungsten Concentrates (GB/T14352.1-2010). And the mass fraction of $WO_3$ in leaching residue was determined according to the Chemical Analysis Method for High-Impurity Tungsten Ores-Secondary Separation-Ignition Gravimetric Method (GB/T 26019-2010).

### 3.3 Experimental results and discussion

**3.3.1 Effect of oxalic acid molar concentration.** In each leaching experiment, the dosage of scheelite was fixed at 10 g, and the leaching conditions were controlled as follows: reaction temperature of 60 °C, reaction time of 6 h, liquid–solid ratio of 20 : 1, and stirring speed of 100 rpm. The effect of varying $H_2C_2O_4$ molar concentration on the $WO_3$ leaching rate from scheelite was investigated, and the results are shown in Fig. 5.

It can be seen from Fig. 5 that the $H_2C_2O_4$ molar concentration has a significant impact on the $WO_3$ leaching rate from scheelite. When the $H_2C_2O_4$ concentration is 1.0 mol $L^{-1}$, the $WO_3$ leaching rate is only 88.86%, with a relatively high residual $WO_3$ content of 11.68% in the leaching residue. With the continuous increase of $H_2C_2O_4$ concentration, the $WO_3$ leaching rate gradually increases. When the $H_2C_2O_4$ concentration is increased to 2.2 mol $L^{-1}$, the $WO_3$ leaching rate reaches 99.15%, and the residual $WO_3$ content in the leaching residue decreases to 0.97%.Meanwhile, the pH value also changes during the decomposition of scheelite with oxalic acid. When the oxalic acid concentration is 2.2 mol $L^{-1}$, the initial pH value of the reaction is 0.35. After the decomposition reaction is complete, the final pH value increases to 2.0, mainly due to the consumption of a large amount of free oxalic acid during the

decomposition process. Subsequently, further increasing the $H_2C_2O_4$ molar concentration leads to a slight change in the $WO_3$ leaching rate from scheelite. Therefore, the optimal $H_2C_2O_4$ concentration is preferably controlled at 2.2 mol $L^{-1}$.

And it can be seen from Fig. 6, at lower molar concentrations of oxalic acid (1.0 mol $L^{-1}$ and 1.4 mol $L^{-1}$), the main phases in the leaching residue were $CaWO_4$, $CaC_2O_4 \cdot H_2O$, $CaMoO_4$, and $WO_3 \cdot 0.5H_2O$, indicating that the decomposition reaction is not fully progressed. At a molar concentration of 1.8 mol $L^{-1}$ oxalic acid, the main phases in the decomposition residue are $CaC_2O_4 \cdot H_2O$ and $H_2WO_4$, indicating that the decomposition reaction is promoted, and there is no significant peak of $CaWO_4$ in the leaching residue. At higher molar concentrations of oxalic acid (2.2 mol $L^{-1}$), the main phase in the leaching residue is $CaC_2O_4 \cdot H_2O$, with no obvious peaks of $CaWO_4$ or $H_2WO_4$, indicating that the decomposition reaction is more fully progressed. Based on the experimental results, it can be concluded that changes in the molar concentration of oxalic acid have a significant impact on the decomposition products, which is consistent with the results of thermodynamic analysis.

The leaching of scheelite with $H_2C_2O_4$ involves multiple steps. Firstly, $H_2C_2O_4$ dissolves in the solution and ionizes to produce free $H^+$ and $C_2O_4^{2-}$ ions. Secondly, the free $H^+$ ions react with $CaWO_4$ in scheelite to generate intermediate $H_2WO_4$, while releasing free $Ca^{2+}$ ions. Thirdly, the free $Ca^{2+}$ ions combine with $C_2O_4^{2-}$ ions to form $CaC_2O_4 \cdot H_2O$ precipitates, which enter the leaching residue. Finally, the intermediate $H_2WO_4$ combines with $C_2O_4^{2-}$ ions to form a highly soluble complex $H_2[WO_3(C_2O_4) \cdot H_2O]$,[17,18] thereby achieving the leaching of $WO_3$. To promote the progress of the leaching reaction, it is necessary to maintain a relatively high $H_2C_2O_4$ molar concentration.

**3.3.2 Effect of reaction temperature.** In each leaching experiment, the dosage of scheelite was fixed at 10 g, and the leaching conditions were controlled as follows: $H_2C_2O_4$ concentration of 2.2 mol $L^{-1}$, reaction time of 6 h, liquid–solid ratio of 20 : 1, and stirring speed of 100 rpm. The effect of varying reaction temperature on the $WO_3$ leaching rate from scheelite was investigated, and the results are shown in Fig. 7.

It can be seen from Fig. 7 that the increase of reaction temperature is beneficial to promoting the leaching of scheelite. When the reaction temperature is 40 °C, the $WO_3$ leaching rate from scheelite is only 96.51%, and the residual $WO_3$ content in the leaching residue reaches 3.79%, which seriously affects the recovery of tungsten. When the leaching temperature is increased to 80 °C, the $WO_3$ leaching rate reaches 99.57%, and the residual $WO_3$ content in the leaching residue decreases from the original 3.79 to 0.49%, which significantly improves the recovery rate of tungsten. Further increasing the reaction temperature to 90 °C results in almost no change in the $WO_3$ leaching rate. Therefore, the optimal reaction temperature is controlled at 80 °C.

**3.3.3 Effect of reaction time.** In each leaching experiment, the dosage of scheelite was fixed at 10 g, and the leaching conditions were controlled as follows: $H_2C_2O_4$ concentration of 2.2 mol $L^{-1}$, reaction temperature of 80 °C, liquid–solid ratio of 20 : 1, and stirring speed of 100 rpm. The effect of varying reaction time on the $WO_3$ leaching rate from scheelite was investigated, and the results are shown in Fig. 8.

It can be seen from Fig. 8 that when the reaction time is 5 h, the $WO_3$ leaching rate from scheelite has reached 99.54%, and the residual $WO_3$ content in the leaching residue is only 0.53%. When the reaction time is shortened to 4 h, due to insufficient leaching reaction, $CaWO_4$ in scheelite is not fully leached by $C_2H_2O_4$, resulting in the decrease of $WO_3$ leaching rate from 99.54 to 98.43%, and the increase of residual $WO_3$ content in the leaching residue from 0.53 to 1.75%. Increasing the reaction time to 6 h or 7 h leads to no obvious change in the $WO_3$ leaching rate. Therefore, the optimal reaction time is preferably 5 h, under which the scheelite leaching can be carried out sufficiently.

**3.3.4 Effect of reaction liquid–solid ratio.** In each leaching experiment, the dosage of scheelite was fixed at 10 g, and the leaching conditions were controlled as follows: $H_2C_2O_4$ concentration of 2.2 mol $L^{-1}$, reaction temperature of 80 °C, reaction time of 5 h, and stirring speed of 100 rpm. The effect of varying reaction liquid–solid ratio on the $WO_3$ leaching rate from scheelite was investigated, and the results are shown in Table 2.

It can be seen from Table 2 that when the reaction liquid–solid ratio is 5 : 1, the scheelite leaching effect is poor, with a $WO_3$ leaching rate of only 88.52% and a high residual $WO_3$ content of 9.79% in the leaching residue. This is mainly because when the liquid–solid ratio is low, the concentrations of total free $H^+$ and $C_2O_4^{2-}$ in the leaching system decrease rapidly, which is not conducive to the leaching of scheelite. When the reaction liquid–solid ratio is increased to 15 : 1, the $WO_3$ leaching rate increases from 88.52 to 99.51%, and the residual $WO_3$ content in the leaching residue decreases from 9.79 to 0.54%. This indicates that a relatively high concentration of free $H^+$ and $C_2O_4^{2-}$ has been maintained in the leaching system, promoting the leaching of scheelite. Subsequently, further increasing the reaction liquid–solid ratio results in no significant change in the scheelite leaching effect. In summary, it is appropriate to control the reaction liquid–solid ratio at 15 : 1.

**3.3.5 Mechanism analysis of scheelite leaching with oxalic acid.** Under the optimal conditions, the scheelite leaching experiment with $H_2C_2O_4$ was carried out: the dosage of scheelite was 50 g, the $H_2C_2O_4$ concentration was 2.2 mol $L^{-1}$, the reaction temperature was 80 °C, the reaction time was 5 h, the reaction liquid–solid ratio was 15 : 1, and the stirring speed was 100 rpm. After the completion of leaching, the mass of leaching residue was 26.25 g, and the residual $WO_3$ content in the leaching residue was 0.49%. XRD, EDS, and FTIR were used to characterize the changes in composition and phase of scheelite before and after $H_2C_2O_4$ leaching, and the mechanism of scheelite leaching with $H_2C_2O_4$ was analyzed, as shown in Fig. 9, 10, and 11.

It can be seen from the XRD patterns in Fig. 9(a) and 8(b) that the main phases in scheelite are $CaWO_4$ and $CaMoO_4$. After leaching with $H_2C_2O_4$, the main phase in the leaching residue is $CaC_2O_4 \cdot H_2O$, and no $CaWO_4$ or $CaMoO_4$ phases are detected, indicating that the leaching reaction proceeds sufficiently.

From the EDS patterns in Fig. 10(a) and (b), it is observed that after scheelite is leached with $H_2C_2O_4$, the content of C element increases from the original 8.06 to 15.38%, the content of W element decreases from 48.78 to 0.15%, and the content of Ca element increases from 15.77 to 29.27%. This phenomenon indicates that most of the tungsten enters the leaching solution in a highly soluble form after the scheelite is leached with $H_2C_2O_4$, while most of the $Ca^{2+}$ ions combine with part of the $C_2O_4^{2-}$ ions to form new precipitates, which remain in the leaching residue.

As shown in the FTIR spectrum of Fig. 11(a), the characteristic absorption peaks of scheelite are mainly derived from the vibration of $WO_4^{2-}$ tetrahedra. The strong absorption peak in the range of 800–900 $cm^{-1}$ corresponds to the asymmetric stretching vibration of the W–O bond, which is the core qualitative peak of $CaWO_4$. The weak absorption peak at 400–500 $cm^{-1}$ is attributed to the bending vibration of O–W–O, which further confirms the existence of $WO_4^{2-}$ ions. From the FTIR spectrum of Fig. 11(b), it can be seen that the strong absorption peak of the $H_2C_2O_4$ leaching residue in the range of 1600–1700 $cm^{-1}$ corresponds to the asymmetric stretching vibration of C=O in oxalate ions. The absorption peaks in the ranges of 1300–1400 $cm^{-1}$ and 1000–1100 $cm^{-1}$ are attributed to the C–O stretching vibration and C–C stretching vibration, respectively. The absorption peaks at 800–900 $cm^{-1}$ and 1200–1300 $cm^{-1}$ are the in-plane and out-of-plane bending vibrations of O–C–O, while the weak absorption peak at 400–500 $cm^{-1}$ corresponds to the lattice vibration of Ca–O. These characteristic peaks indicate that the main component of the $H_2C_2O_4$ leaching residue is calcium oxalate.

In summary, during the process of scheelite leaching with $H_2C_2O_4$, tungsten enters the solution in the form of a highly soluble complex ($H_2[WO_3(C_2O_4)\cdot H_2O]$), while calcium remains in the leaching residue as calcium oxalate precipitate ($CaC_2O_4\cdot H_2O$).

# 4 Conclusion

(1) The equilibrium diagram of the Ca–W–Oa–$H_2O$ system for the $H_2C_2O_4$ leaching of scheelite at 298 K was constructed. The dominant regions of each component in the system and the variations of key components with pH value and total concentration of free $H_2C_2O_4$ were analyzed. The results indicate that the concentration of free $H_2C_2O_4$ is a crucial factor affecting the leaching efficiency. When $1 < pH < 6.4$, scheelite can react with $H_2C_2O_4$ to form precipitates of $H_2WO_{4(s)}$ and $CaC_2O_{4(s)}$. Moreover, maintaining a high concentration of free $H_2C_2O_{4(aq)}$ can promote the leaching of scheelite. When $6.4 < pH < 14.6$, the ionization of $H_2C_2O_4$ is enhanced with the increase of pH, resulting in the elevation of $C_2O_4^{2-}$ and $WO_4^{2-}$ concentrations. When $pH > 14.6$, the binding interaction between $OH^-$ and $Ca^{2+}$ in the system is drastically strengthened, and $CaC_2O_{4(s)}$ is gradually converted into $Ca(OH)_{2(s)}$.

(2) Experimental validation of $H_2C_2O_4$ leaching for scheelite was carried out. Under the optimized conditions of an $H_2C_2O_4$ concentration of 2.2 mol $L^{-1}$, reaction temperature of 80 °C, reaction time of 5 h, liquid-to-solid ratio of 15 : 1, and stirring speed of 100 rpm, the leaching rate of $WO_3$ reached 99.54%, with the $WO_3$ content in the leaching residue as low as 0.53%. A comparative analysis of the XRD, EDS, and FTIR characterization results of raw scheelite and $H_2C_2O_4$-leached scheelite residue indicated that during the leaching process, most of the tungsten entered the leachate in the form of $H_2[WO_3(C_2O_4\cdot H_2O)]$ (a highly soluble species), while calcium combined with $C_2O_4^{2-}$ to form $CaC_2O_4\cdot H_2O$ precipitate, which was retained in the leaching residue.

# Author contributions

Ting Xie: conducted all the scheelite leaching experiments, collected and analyzed the experimental data, participated in the characterization analysis of leaching samples, and drafted the original manuscript. Jisen Huang: proposed the research topic and research hypothesis, designed the scheelite leaching experiment scheme and characterization test plan. Bin Zeng: critically revised the manuscript for important intellectual content, and provided financial support for the whole research project. Xiangrong Zeng: carefully revised and polished the manuscript, including language expression, logical structure and academic specification. Chong Peng: provide experimental raw materials and methods, and offer theoretical guidance, reviewed the final manuscript. Zhonghua Wang: guided the experimental design and mechanism analysis, put forward valuable suggestions for the optimization of leaching conditions, and reviewed the final manuscript.

# Conflicts of interest

The authors declare that they have no competing interests.

# Data availability

The datasets used and/or analysed during the current study are available from the corresponding author on reasonable request.

# Acknowledgements

This research was financially supported by the Key Research and Development Program of Jiangxi Province(20244BBG73010), the Natural Science Foundation of Jiangxi Province(2024BAB28054), the Project Supported by the Natural Science Foundation of Jiangxi Province(20242BAB25244), the Science and Technology Achievement Maturation and Engineering Project of Ganzhou(2024SHCC0015), the High level and High skilled Leading Talent Training Project of Jiangxi Province (Gan Ren She Fa [2023] No. 179).

# References

1 F. Sun, Z. Fu and Z. Zhao, Development of Tungsten-Molybdenum Separat ion Technology, *Nonferrous Met.*, 2025, (9), 1–12.

2 H. Li, *Rare Metal Metallurgy*, Beijing, Metallurgical Industry Press, 1990, pp. 54–56.
3 Z. Zhao, F. Sun, J. Yang, Q. Fang, W. Jiang, X. Liu, X. Chen and J. Li, Status and prospect for tungsten resources, technologies and industrial development in China, *Chin. J. of Nonferrous Met.*, 2019, **29**(9), 1902–1916.
4 P. Tang, J. Wang and Y. Zhou, Analysis of the current situation of global tungsten resources and suggestions, *China Min. Mag.*, 2016, **25**(Suppl.1), 9–12.
5 Y. Gao, Tungsten resource characteristics of China and research advances of tungsten processing technologies, *China Tungsten Ind.*, 2016, **31**(5), 35–39.
6 B. Zeng, X. Zeng and W. Huang, Study on Leaching Molybdenum and Tungsten Processes of Phosphorus Removal Slag from Tungsten Smelting, *Mater. Rep.: Energy*, 2023, **37**(15), 207–211.
7 Z. Zhao, Y. Liang, X. Liu, A. Chen and H. Li, Sodium hydroxide digestion of scheelite by reactive extrusion, *Int. J. Refract. Met. Hard Mater.*, 2011, **29**(6), 739–742.
8 J. P. Martins and F. Martins, Soda ash leaching of scheelite concentrates: the effect of high concentration of sodium carbonate, *Hydrometallurgy*, 1997, **46**(1), 191–203.
9 L. Wan, *Tungsten Metallurgy*, Beijing: Metallurgical Industry Press, 2011.
10 Z. Zhao, *Tungsten Metallurgy: Fundamentals and Applications*, Beijing, Tsinghua University Press, 2013, pp. 21−28.
11 H. Li, J. Yang and K. Li, *Tungsten Metallurgy*, Changsha, Central South University Press, 2010, 53–112.
12 K. Yang, W. Zhang, L. He, Y. Li, F. Guo, X. Chen, J. Li, X. Liu and Z. Zhao, Leaching kinetics of wolframite with sulfuric-phosphoric acid, *Chin. J. of Nonferrous Met.*, 2018, **28**(1), 175–182.
13 J. Li and Z. Zhao, Kinetics of scheelite concentrate digestion with sulfuric acid in the presence of phosphoric acid, *Hydrometallurgy*, 2016, **163**, 55–60.
14 G. Xu, D. Yu and Y. Su, Leaching of scheelite by hydrochloric acid in the presence of phosphate, *Hydrometallurgy*, 1986, **16**(1), 27–40.
15 X. Wang, J. Li, W. Zhang, G. He and Z. Zhao, Decomposition of synthetic scheelite in HCl solution with hydrogen peroxide as complexing agent, *Chin. J. of Nonferrous Met.*, 2014, **24**(12), 3142–3146.
16 X. Liu, J. Xiong, X. Chen, J. Li, L. He, F. Sun and Z. Zhao, Acidic decomposition of scheelite by organic sodium phytate at atmospheric pressure, *Miner. Eng.*, 2021, **172**, 107125.
17 W. Zhang, Y. Chen, J. Che, C. Wang and B. Ma, Green leaching of tungsten from synthetic scheelite with sulfuric acid-hydrogen peroxide solution to prepare tungstic acid, *Sep. Purif. Technol.*, 2020, **241**, 116752.
18 Q. Liu, T. Tu, H. Guo, H. Cheng and X. Wang, Complexation extraction of scheelite and transformation behaviour of tungsten-containing phase using $H_2SO_4$ solution with $H_2C_2O_4$ as complexing agent, *Trans. Nonferrous Met. Soc. China*, 2021, **31**(10), 3150–3161.
19 Z. Chen, Y. Liu, Y. Liang, T. Pu and W. Lai, Study on the law and mechanism by which $H_2C_2O_4$ dissolves tungstic acid, *BMC Chem.*, 2025, **19**(1), 149.
20 Y. M. Potashnikov, A. M. Gamol'Skii and M. V. Mokhosoev, Kinetics of the dissolution of calcium tungstate in oxalate acid solution, *Zh. Neorg. Khim.*, 1970, **15**(2), 502–508.
21 A. Kalpakli, S. Ilhan, C. Kahruman and I. Yusufoglu, Dissolution behavior of calcium tungstate in $H_2C_2O_4$ solutions, *Hydrometallurgy*, 2012, **121–124**, 7–15.
22 C. Cao, Z. Peng, H. Lu, Y. Lv and A. Fu, Thermodynamic analysis on decomposition of calcium oxalate with acid, *J. Cent. South Univ.*, 2023, **54**(2), 422–430.
23 X. Liu, X. Zhu, X. Chen, J. Li, L. He, F. Sun and Z. Zhao, Thermodynamic analysis of scheelite decomposition by sodium phytate, *Chin. J. of Nonferrous Met.*, 2022, **32**(2), 529–535.
24 W. Zhang, B. Ma and C. Wang, Thermodynamics analysis on formation of calcium arsenate slag, *Nonferrous Met.*, 2019, (9), 61–66.
25 Z. Ding and Z. Zhao, Thermodynamic analysis of scheelite leaching by fluoride solution, *Rare Met. Cem. Carbides*, 2004, **32**(1), 8–10.
26 C. Cao, Z. Zhao, X. Liu and X. Wang, Thermodynamic study on decomposition of scheelite with sodium silicate, *Chin. J. of Nonferrous Met.*, 2012, **22**(9), 2636–2641.
27 J. Li, Thermodynamic Analysis of Aqueous Solutions in Ammonium Phosphate-Ammonia System Leaching of Scheelite, *Resource Information and Engineering*, 2018, **33**(3), 96–98.
28 Z. Zhao, C. Cao and H. Li, Thermodynamics on soda decomposition of scheelite, *Chin. J. Nonferrous Met.*, 2008, **18**(2), 356–360.
29 S. Tu, C. Cao and Z. Zhao, Thermodynamic Analysis of EDTA Leaching of Scheelite, *China Tungsten Ind.*, 2011, (3), 27–30.